

# MODIS Brightness Temperature Change-based Forest Fire Monitoring

Fatemeh Parto<sup>1,2\*</sup>, Mohammadreza Saradjian<sup>1</sup>, Saeid Homayouni<sup>3</sup>

1 Remote Sensing Division, School of Surveying and Geospatial Engineering, College of Engineering, University of Tehran, Tehran, Iran.

2 Geodesy and Geomatics Faculty, K.N.Toosi University of Technology, Tehran, Iran.

3 Centre Eau Terre Environment, Insitut National de la Recherche Scientifique, Québec, Canada

\* Corresponding authors: fparto.id@gmail.com

## Abstract

Forests, as one of the most important natural resources in the world, are facing several challenges due to human activities and climate changes. The timely detection of forest fires plays an essential role in managing this wealth. Despite several well-developed fire detection methods, the detection of fires in early hours is still challenging. In this paper, we developed a new near-real-time hybrid method for fire detection that has high sensitivity to small and cold forest fires as well as less rate of false alarms. This method is based on detecting of both spatial and temporal changes. The change detection technique was used, and the identification of fire pixels was performed in the area with a significant change compared to the previous time. Since most of the false fire pixels had almost the same temperature in the images, they were masked. This mask allowed us to reduce the fire thresholds that lead to detect small fires. Furthermore, the omission and commission errors were minimized. This algorithm was applied to forty case studies in the north of Iran. The identified fire pixels were validated with ground observations collected by The Forests, Range and Watershed Management Organization (FRWMO) of Iran. Results show that the proposed algorithm was able to detect small and cool-case fires efficiently.

**Keywords:** Change Detection, Environment Management, Fire Detection, MODIS, Remote Sensing.

## 36 **1. Introduction**

37 The Moderate Resolution Imaging Spectroradiometer (MODIS) is an instrument on the Terra  
38 and Aqua satellites which observes the Earth's surface every 1-2 days in 36 spectral bands.  
39 Instrument proficiency has been emphasized since the launch, and several fire detection methods  
40 based on MODIS imagery were proposed. These algorithms are mostly dependent on spatial hot  
41 spot detection using thermal infrared (TIR) bands.

42 Despite several algorithms for detecting fire, much remains to be considered to monitor the fire  
43 precisely. Kaufman et al. developed a MODIS algorithm for fire detection that set different  
44 thresholds for fires (Kaufman et al. 1998). Giglio et al. improved several aspects of this  
45 algorithm and proposed a contextual fire detection algorithm that has high sensitivity in  
46 detecting fire pixels (Giglio et al. 2003). MODIS Collection 4 Active Fire Products are based  
47 on this algorithm. Subsequently, this algorithm has been used in many studies (e.g., Chuvieco  
48 et al. 2008; Li et al. 2000; Cheng et al. 2013). For instance, Cheng et al. evaluated the MODIS  
49 product in the Yucatán Peninsula. They realized that omission errors were mainly caused by  
50 the potential fire threshold and reduced the daytime threshold to 305 K (Cheng et al. 2013).  
51 Moreover, examining the firing thresholds in the southeastern United States indicated that some  
52 fire pixels had brightness temperatures below the daytime potential fire threshold (Wang et al.  
53 2006).

54 Consequently, Giglio et al. developed an enhanced algorithm for fire detection that overcomes  
55 some limitations in the previous algorithm (Giglio et al. 2016). In this algorithm, they identified  
56 areas that are susceptible to fires and reduced thresholds in these areas. The results indicated  
57 that this new fire detection algorithm had been improved compared to the previous one, with  
58 lower omission errors and false alarms. MODIS Collection 6 Active Fire Products are based  
59 on this developed algorithm. This algorithm has shown an efficient performance in several  
60 cases e.g. Furnacca et al. (2017); Abdollahi et al. (2018).

61 Wang used smoke bands and performed fire detection in the smoke area based on the smoke  
62 transmission radius. This algorithm can detect small and cold fires, especially at large scan  
63 angles, but it has a limitation in the non-smoke fire areas (Wang et al. 2009).

64 Although the efficient performance of the Giglio algorithm, still there are some limitations in  
65 detecting small fires. In the current study, we proposed a new forest fire detection algorithm  
66 based on Giglio et al., algorithm and change detection technique that could detect small fires  
67 with more accuracy.

68

## 69 **2. Study area and data set**

### 70 **2.1. Study area**

71 About 8%, or nearly 12.4 million hectares, of the total area of Iran, is covered by forests. Every  
72 year, there are devastating fires in Iran that damage the forest resources. The losses caused by  
73 forest fires are irrecoverable. The season of fire varies depending on humidity, wind, location  
74 and climatic conditions. In the northern part of Iran, we have most fires from August to the end  
75 of December. While most fires in the eastern part of the country happen in summer and winter.  
76 Golestan forest is located next to the Caspian Sea area. It has the most critical forest fields.  
77 Fifty-two fires were reported there in 1998. Based on (Ardakani et al. 2011.), 86.21% of the  
78 fires detected by MODIS images occurred in cropland, grassland, and plain regions. Most of  
79 these fires have occurred in the eastern regions of the Caspian Sea. So we concentrated on this  
80 area.

### 81 **2.2. Satellite data**

82 The remote sensing data that used in this study consisted of MODIS Level 1B Radiance product  
83 (MOD021/MYD021) and the geolocation dataset (MOD03/MYD03). These data were  
84 obtained from the Earth Observing System Data Gateway, Land Processes Distributed Active  
85 Archive Centre (DAAC). The fires information was collected by The Forests, Range and  
86 Watershed Management Organization (FRWMO) of Iran and used to evaluate the results. Each  
87 forest fire case contains information on the initial and extinguishing time, location, and  
88 damaged area. The MOD03 was used to georeference the MOD021 Images. The atmospheric  
89 correction was performed using Flash software. Then the ‘‘bowtie’’ effect or overlap between  
90 MODIS scans corrected by the Wen algorithm (Wen et al. 2008). Later the radiances were  
91 converted to brightness temperatures by Planck's Radiation Law. Then, in order to reduce the  
92 stripping error, the de-stripping tools in ENVI were used. Furthermore, the steps of the algorithm  
93 were done and then results validated with ground data.

## 94 **3. Proposed Algorithm**

95 In the proposed algorithm, based on the maximum sensitivity, MODIS 3.9 and 11  $\mu\text{m}$  channels  
96 were used to detect fire pixels in images. These channels are denoted by T3.9 and T11. The  
97 250-1000 m resolution red and near-infrared channels were used to mask clouds, water and  
98 calculation of the Normalized Difference Vegetation Index (NDVI) index.  
99 Our algorithm reached to high accuracy in four steps: first, masked out the water pixels based  
100 on the NDVI index. Second, removed the pixels which cause false alarms in boundaries by

101 using dilation and closing morphological operation. Third, applied the change mask, which was  
 102 performed, based on the pixel temperature difference of two consecutive images. This phase  
 103 had a considerable enhancement in detecting small fires because it allowed reducing the fire  
 104 thresholds. Finally, excluded the phase of false alarm rejection that removed some of the small  
 105 and cold fires. The change mask phase removed most of the false alarm pixels due to the same  
 106 situation of them in both images without omitting small fire pixels. The procedure of the  
 107 proposed fire detection algorithm is described below.

### 108 **3.1. Cloud and Water Masking**

109 In this phase, channels 1, 2, 31 and 32 were used for the identification of cloud pixels. The  
 110 pixel that satisfies the following tests is considered as cloudy pixels (Giglio et al. 2003.):

$$111 \quad (\rho_{0.65} + \rho_{0.85} > 0.9) \text{ or } (T_{12} < 265 \text{ K}) \text{ or } (\rho_{0.65} + \rho_{0.85} > 0.7) \text{ and } (T_{12} < 285 \text{ K})$$

112 For the night image:

$$113 \quad T_{12} < 265 \text{ K}$$

114 False alarms appeared in the cloud boundaries due to the low potential fire threshold.  
 115 Accordingly, the dilation and closing of morphological operations were applied to the cloud  
 116 mask to remove the cloud edge and gaps. Then, a water mask based on the NDVI index was  
 117 performed on the images. Pixels with  $\text{NDVI} < 0.05$  were considered as water pixels.

$$118 \quad \text{NDVI} = \frac{\text{NIR} - R}{\text{NIR} + R}$$

### 119 **3.2. Change Detection**

120 Change detection is a technique to determine those pixels on images that have changed  
 121 compared to the previous ones. Various environmental factors can change different aspects of  
 122 pixels. This technique defines a threshold value to identify areas of “change” and “no change”  
 123 pixels in the image.

124 In the proposed method, fire detection was performed on the pixels with noticeable brightness  
 125 temperature changes over time that was recognized by a preliminary classification based on  
 126 change detection. "No change" pixels are non-fire pixels, even if they have a high temperature,  
 127 like hot desert pixels. In this phase, a change mask was applied to thermal bands between two  
 128 images. Pixels with lower-threshold temperatures were classified as non-fire pixels. This  
 129 threshold, which is denoted by  $Td$  is set dynamically based on the average temperature  
 130 difference of two images:

131 
$$T_d = \frac{\bar{T}_4^2 - \bar{T}_4^1}{3}$$

132 This mask eliminated the pixels with small changes in brightness temperature. Many of pixels  
 133 that constructed commission errors in previous works were removed at this stage because they  
 134 almost had the same situation in both images. As a result, fire detection was applied to the  
 135 pixels that have changed in thermal bands over time.

### 136 **3.3. Detection of Fire Pixels**

137 There are three logical stages through which fire pixels can be identified; i) detection of  
 138 potential fire pixels, ii) absolute test, and iii) relative test. In the first step, a daytime pixel was  
 139 identified as a potential fire pixel if  $T_{3.9} > T_{d1}$ ,  $T_{3.9} - T_{11} > T_{d2}$  and  $p_{.86} < 0.3$ .

140 Thresholds are identified based on  $T_{d1}$  and  $T_{d2}$ . They set dynamically according to the  
 141 brightness temperature of the pixels in the image. This way was suggested by (Zhukov et al.  
 142 2006). They calculated the thresholds based on the following equations:

143 
$$T_{d1} = \text{average}(T_{3.9})_j + 5K$$

144 
$$T_{d2} = \text{average}(T_{3.9} - T_{11})_j + 5k$$

145 Where  $j$  is the sample position in the range of ( $0 \leq j \leq 1353$ ). The pixels that passed these tests  
 146 were classified as potential-fire pixels and considered in some tests to detect active fire pixels  
 147 and those remained pixels were considered as non-fire pixels.

148 In the second step, the pixels containing active fires were identified. This threshold was set to  
 149 the value 360/320 for day-/night-time, respectively (Kaufman et al. 1998).

150 
$$T_4 > 360K$$

152 
$$T_4 > 320K \quad (1)$$

154 In the third phase, after detecting the spatial thermal variations, the relative tests were applied.  
 155 The pixels around the potential fire pixel were used to estimate the background value. Within  
 156 a window, the valid pixels are defined as those pixels which are located on the ground, do not  
 157 contain cloud and subject to the following conditions:

158  $T_{3.9} < 315K$  or  $T_{3.9} - T_{11} < 9.5K$  for daytime, and  $T_{3.9} < 305K$  or  $T_{3.9} - T_{11} > 9.5K$  for  
 159 nighttime. Notably, we reduced the thresholds of this stage compared to (Giglio et al. 2003).

160 The window starts as a  $3 \times 3$  pixel and is maximized to  $10 \times 10$  pixels as needed. In the conditions  
 161 that at least four of the valid neighboring pixels could be identified, some measures were  
 162 calculated. A summary of this process is presented in Table 1.

163

164

165 Table1. Summary of the background pixels parameters (Giglio et al. 2003)

Parameter	Description
$\bar{T}_4$	mean of T3.9 for the valid neighboring pixels
$\delta_4$	mean absolute deviation of T3.9 for the valid neighboring pixels
$\bar{T}_{11}$	mean of T11 for the valid neighboring pixels
$\delta_{11}$	mean absolute deviation of T11 for the valid neighboring pixels
$\bar{T}_{\Delta T}$	mean of T3.9–T11 for the valid neighboring pixels
$\delta_{\Delta T}$	mean absolute deviation of T3.9–T11 for the valid neighboring pixels

166

167 In the relative tests, both the 3.9  $\mu\text{m}$  brightness temperature (T3.9) and the 3.9 and 11  $\mu\text{m}$   
 168 brightness temperature difference ( $\Delta T$ ) was used. Relative thresholds were determined based  
 169 on the natural changes in the background. These tests are defined as follows:

170

$$171 \Delta T > \Delta T + 3.5\sigma_{\Delta T} \quad (2)$$

$$172 \Delta T > \Delta T + 6K \quad (3)$$

$$173 T_4 > \bar{T}_4 + 3\sigma_4 \quad (4)$$

$$174 T_{11} > \bar{T}_{11} + \sigma_{11} \quad (5)$$

$$175 \sigma_{11} > 5k \quad (6)$$

176 A daytime pixel is classified as a fire pixel if (test (1) is true) or (tests (2)-(4) are true and one  
 177 of the tests of (5) or (6)). Otherwise, it is classified as non-fire.

178 A night-time fire pixel is classified as fire if test (1) is true or tests (2)-(4) are true; otherwise,  
 179 it is classified as non-fire (Giglio et al. 2003).

180 The schematic illustration of the proposed algorithm is shown in Fig. 1.

181

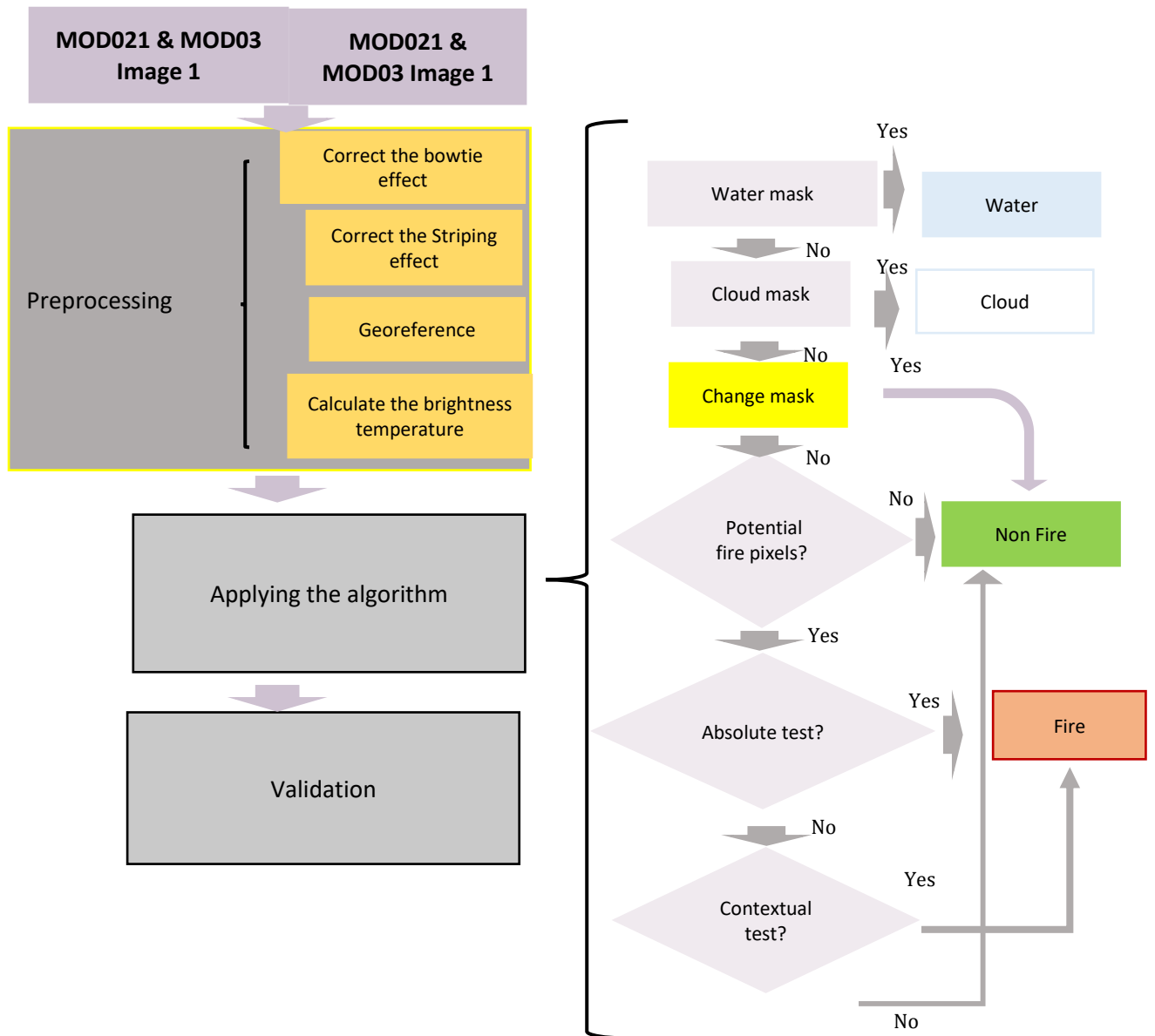


Fig. 1. Flowchart of the proposed fire detection algorithm

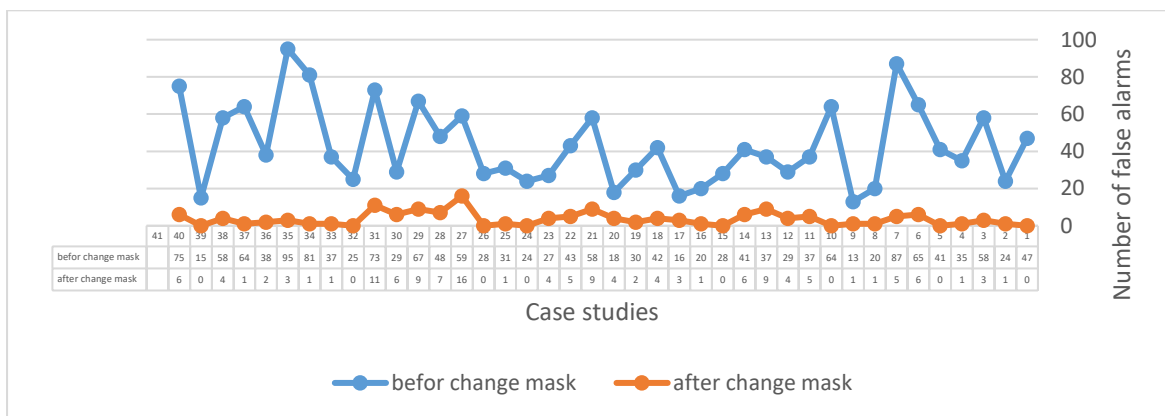
#### 4. Result and Discussion

In this paper, we proposed a new hybrid fire detection method based on both spatial and temporal changes. Fuel type and weather conditions have a significant influence on predisposing an area. Consequently, some improvements must be made for small fire detection on a regional scale and the potential fire threshold should be defined low enough. However, a lower threshold may increase the number of false alarms. Moreover, the false alarm rejection step in Giglio et al. algorithms eliminates some small fires as well.

To date, most of the exiting omission error reduction techniques increase commission errors and conversely, furthermore the fire detection algorithms are mostly based on analyzing the

195 spatial variation. While investigating temporal variation can significantly enhance the accuracy  
 196 of detection of fire pixels. In our work, this point was considered. It can be seen clearly that  
 197 when a fire occurs in some pixels, their temperature has been changed significantly compared  
 198 to the previous times. So a change mask was exploited in the proposed algorithm, and fire  
 199 pixels were detected among the pixels that had a temperature variation. In particular, the  
 200 proposed algorithm looks for a pixel that is hotter than both its neighborhoods and itself over  
 201 time. This technique removed most of the false alarms without deleting fire pixels.  
 202 Furthermore, this step had a significant enhancement for the small fire detection because the  
 203 fire thresholds could be reduced without increasing the number of false alarms, and both  
 204 commission and omission errors were minimized.  
 205 This algorithm was applied to forty case studies in the eastern regions of the Caspian Sea and  
 206 validated by data collected by the Forests, Range and Watershed Management Organization  
 207 (FRWMO) of Iran. The number of false alarms before and after applying the change mask for  
 208 each case study is shown in Fig. 2.

209



210

211 Fig. 2. Number of false alarms before and after change mask for each case study

212 As an example, the number of false alarms for the first and second images is presented in  
 213 table 2.

214 Table. 2. Effect of each mask on the number of false alarms in the first and second case study

		Before applying the mask	After applying the mask
<b>Water Mask</b>	Image1	97	47
	Image2	51	24
<b>Change Mask</b>	Image1	47	0
	Image2	24	1

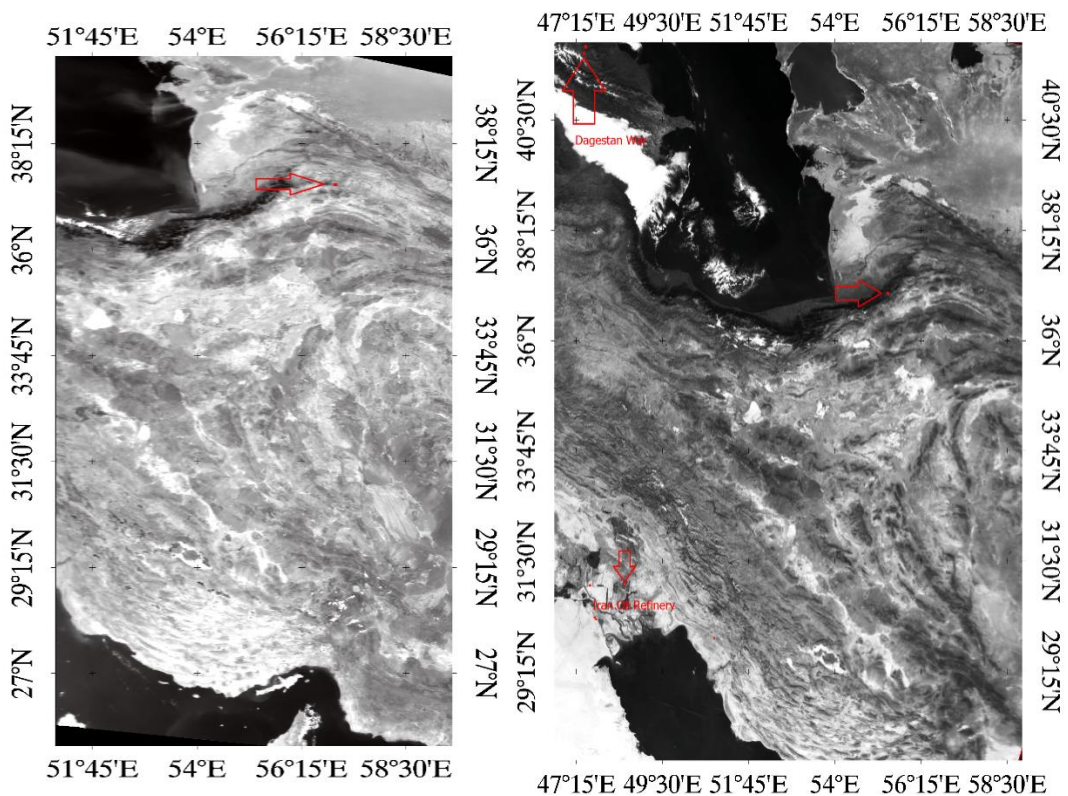
215

216



217 The proposed algorithm detected 39 fires of case studies and some false alarms. Next, the  
 218 Giglio algorithm was applied to these fire images. This algorithm only traversed 32 cases;  
 219 furthermore, the number of false alarms was less than the proposed algorithm in 15 cases. In  
 220 these cases, the second image was checked out, and by replacing the more appropriate one, the  
 221 number of false alarms was decreased. The probability of fire detection in the proposed  
 222 algorithm is strongly dependent on the condition of the second image. Different images as the  
 223 second image with different time intervals were used. Results demonstrate that when the time  
 224 interval between the two images in the change mask was increased, the number of false alarms  
 225 was grown up. Consequently, to achieve high accuracy in this algorithm, the weather condition  
 226 in the second image must be similar to the main image and missing data and cloud pixels should  
 227 be minimal.

228 Examples of detected fires in the first and second case studies are shown in Fig.3.



229  
 230 Fig. 3. An example of detected fires in the first and second case study

### 231 4.1. Accuracy Assessment

232 In order to evaluate this algorithm, Reference-based accuracy, Omission Error, Map-based  
 233 accuracy and Commission Error were calculated:

- 234 - Reference-based accuracy or Producer's accuracy is obtained by the ratio of the number  
 235 of correct pixels into the total number of pixels in a class.

236 *Producer's accuracy = classified pixels in the specified class/ground reference pixels in this class*

237 - Omission Error means a pixel that should have been included in the class:

238 
$$\text{Omission Error} = 1 - \text{Producer's accuracy}$$

239 - Map-based accuracy or User's accuracy that determining the percentage of correct  
240 predictions:

241 
$$\text{User's accuracy} = \frac{\text{correctly classified pixels as a specified class}}{\text{total of classified pixels as the this specified class}}$$

243 - Commission Error means including a pixel in a class when it had to be removed:

244 
$$\text{Commission Error} = 1 - \text{User's accuracy}$$

245 These parameters and values obtained from the proposed algorithm and the Giglio algorithm  
246 are presented in table 3.

247 Table. 3. Effect of each mask on the number of false alarms in the first and second case study

Parameter	First Case Study	Second Case Study
<b>Producer's accuracy</b>	93.5%	80%
<b>Omission Error</b>	2.5%	20%
<b>User's accuracy</b>	89%	95.5%
<b>Commission Error</b>	11%	4.5%

## 248 5. Conclusion

249 We have developed an appropriate platform for small and cold fire detection. One of the crucial  
250 reasons for false alarms in previous works was water pixels. Consequently, in the currently  
251 proposed algorithm, we masked out the water pixels using the NDVI index. After that, a  
252 dilation and closing morphological operation were used to remove the pixels, which cause false  
253 alarms in boundaries. The result showed that the proposed algorithm had no false alarm from  
254 water pixels in the case studies. The milestone of this study was to identify the hot spots based  
255 on both temporal and spatial changes. A change mask was applied to the fire image, which was  
256 performed based on the difference between thermal bands of two images. This mask allowed  
257 us to reduce the fire thresholds to a regional low and cold fire temperature and had a  
258 considerable enhancement in detecting fires in early hours, so the omission errors were  
259 minimized.

260 Moreover, our algorithm does not need a false alarm rejection step which is considered as one  
261 of the main phases in MODIS Active Fire algorithms and omitted some of the small and cold  
262 fires, because the change mask removed most of these false alarm pixels without deleting fire  
263 pixels since they had the same situation in both images without omitting small fire pixels.  
264 Therefore, It leads to a decreasing in commission errors. Together, our results indicated that  
265 the proposed method had a good improvement for identifying fires in the first hours to prevent  
266 it from spreading and had a notable improvement to minimize commission and omission errors.

## 267 6. Acknowledgment

268 We thank Forests, Range and Watershed Management Organization (FRWMO) of Iran for  
269 trooping ground observations and Earth Observing System Data Gateway, Land Processes  
270 Distributed Active Archive Centre (DAAC) for providing MODIS data.

## 271 7. References

- 272 Abdollahi, M., Islam, T., Gupta, A., & Hassan, Q. (2018). An Advanced Forest Fire Danger Forecasting  
273 System: Integration of Remote Sensing and Historical Sources of Ignition Data. *Remote Sensing*,  
274 *10*(6), 923. <https://doi.org/10.3390/rs10060923>
- 275 Ardakani, A. S., Zoej, M. J. V., Mohammadzadeh, A., & Mansourian, A. (2011). Spatial and Temporal  
276 Analysis of Fires Detected by MODIS Data in Northern Iran From 2001 to 2008. *IEEE Journal*  
277 *of Selected Topics in Applied Earth Observations and Remote Sensing*, *4*(1), 216–225.  
278 <https://doi.org/10.1109/JSTARS.2010.2088111>
- 279 Cheng, D., Rogan, J., Schneider, L., & Cochrane, M. (2013). Evaluating MODIS active fire products  
280 in subtropical Yucatán forest. *Remote Sensing Letters*, *4*(5), 455–464.  
281 <https://doi.org/10.1080/2150704X.2012.749360>
- 282 Chuvieco, E., Giglio, L., & Justice, C. (2008). Global characterization of fire activity: toward defining  
283 fire regimes from Earth observation data. *Global Change Biology*, *14*(7), 1488–1502.  
284 <https://doi.org/10.1111/j.1365-2486.2008.01585.x>
- 285 Fornacca, D., Ren, G., & Xiao, W. (2017). Performance of Three MODIS Fire Products (MCD45A1,  
286 MCD64A1, MCD14ML), and ESA Fire\_CCI in a Mountainous Area of Northwest Yunnan,  
287 China, Characterized by Frequent Small Fires. *Remote Sensing*, *9*(11), 1131.  
288 <https://doi.org/10.3390/rs9111131>
- 289 Giglio, L., Descloitres, J., Justice, C. O., & Kaufman, Y. J. (2003). An Enhanced Contextual Fire  
290 Detection Algorithm for MODIS. *Remote Sensing of Environment*, *87*(2–3), 273–282.  
291 [https://doi.org/10.1016/S0034-4257\(03\)00184-6](https://doi.org/10.1016/S0034-4257(03)00184-6)
- 292 Giglio, L., Schroeder, W., & Justice, C. O. (2016). The collection 6 MODIS active fire detection  
293 algorithm and fire products. *Remote Sensing of Environment*, *178*, 31–41.  
294 <https://doi.org/10.1016/J.RSE.2016.02.054>
- 295 Kaufman, Y. J., Justice, C. O., Flynn, L. P., Kendall, J. D., Prins, E. M., Giglio, L., et al. (1998).  
296 Potential global fire monitoring from EOS-MODIS. *Journal of Geophysical Research:*  
297 *Atmospheres*, *103*(D24), 32215–32238.  
298 [https://doi.org/10.1029/98JD01644@10.1002/\(ISSN\)2169-8996.EOSAM1](https://doi.org/10.1029/98JD01644@10.1002/(ISSN)2169-8996.EOSAM1)
- 299 Li, Z., Kaufman, Y. J., Ichoku, C., Fraser, R. H., Trishchenko, A. P., Giglio, L., et al. (2000). A Review  
300 of AVHRR-based Active Fire Detection Algorithms: Principles, Limitations, and  
301 Recommendations. [https://www.semanticscholar.org/paper/A-Review-of-AVHRR-based-](https://www.semanticscholar.org/paper/A-Review-of-AVHRR-based-Active-Fire-Detection-and-Li-Kaufman/dbed83d5a47f63f377c9c3dbf714b57225f654ca)  
302 [Active-Fire-Detection-and-Li-Kaufman/dbed83d5a47f63f377c9c3dbf714b57225f654ca](https://www.semanticscholar.org/paper/A-Review-of-AVHRR-based-Active-Fire-Detection-and-Li-Kaufman/dbed83d5a47f63f377c9c3dbf714b57225f654ca).  
303 Accessed 6 October 2019
- 304 Movaghati, S., Samadzadegan, F., & Azizi, A. (2008). A COMPARATIVE STUDY OF THREE  
305 ALGORITHMS FOR FOREST FIRE DETECTION IN IRAN.  
306 [https://www.semanticscholar.org/paper/A-COMPARATIVE-STUDY-OF-THREE-](https://www.semanticscholar.org/paper/A-COMPARATIVE-STUDY-OF-THREE-ALGORITHMS-FOR-FOREST-Movaghati-Samadzadegan/c904da8dc83e62a44bc3b494cfbc2fcfd35c4e0e)  
307 [ALGORITHMS-FOR-FOREST-Movaghati-](https://www.semanticscholar.org/paper/A-COMPARATIVE-STUDY-OF-THREE-ALGORITHMS-FOR-FOREST-Movaghati-Samadzadegan/c904da8dc83e62a44bc3b494cfbc2fcfd35c4e0e)  
308 [Samadzadegan/c904da8dc83e62a44bc3b494cfbc2fcfd35c4e0e](https://www.semanticscholar.org/paper/A-COMPARATIVE-STUDY-OF-THREE-ALGORITHMS-FOR-FOREST-Movaghati-Samadzadegan/c904da8dc83e62a44bc3b494cfbc2fcfd35c4e0e). Accessed 6 October 2019
- 309 Wang, W., Hao, X., Liu, Y., & Sommers, W. T. (2007). An improved algorithm for small and cool fire  
310 detection using MODIS data: A preliminary study in the southeastern United States. *Remote*  
311 *Sensing of Environment*, *108*(2), 163–170. <https://doi.org/10.1016/J.RSE.2006.11.009>
- 312 Wang, W., Qu, J. J., Hao, X., & Liu, Y. (2009). Analysis of the moderate resolution imaging  
313 spectroradiometer contextual algorithm for small fire detection. *Journal of Applied Remote*  
314 *Sensing*, *3*(1), 031502. <https://doi.org/10.1117/1.3078426>
- 315 Wen, X. (2008) . A New Prompt Algorithm For Removing The Bowtie Effect Of Modis L1b Data.  
316 Commission III, WG III/1.

317 Zhukov, B., Lorenz, E., Oertel, D., Wooster M., & Roberts, G. (2006). Spaceborne Detection And  
318 Characterization Of Fires During The Bi-Spectral Infrared Detection (BIRD) Experimental Small  
319 Satellite Mission (2001-2004). *Remote Sensing of Environment*, 100, 29–51.